Journal of the Franklin Institute 362 (2025) 107471

Contents lists available at ScienceDirect

Journal of the Franklin Institute

journal homepage: www.elsevier.com/locate/fi

Neural network-based adaptive fault-tolerant control for strict-feedback nonlinear systems with input dead zone and saturation

Mohamed Kharrat [a], Moez Krichen [b,c], Hadil Alhazmi [d], Paolo Mercorelli [e,*]

[a] Mathematics Department, College of Science, Jouf University, Sakaka, Saudi Arabia
[b] Al- Baha University, Al- Bahah 65528, Saudi Arabia
[c] ReDCAD Laboratory, University of Sfax, Sfax 3038, Tunisia
[d] Department of Mathematical Sciences, College of Science, Princess Nourah Bint Abdulrahman University, P.O. Box 84428, Riyadh, 11671, Saudi Arabia
[e] Institute for Production Technology and Systems, Leuphana University of Lueneburg, Lueneburg, 21335, Germany

ARTICLE INFO

Keywords:
Nonlinear system
Adaptive control
Lyapunov function
Actuator fault
Dead-zone
Saturation
One-link manipulator

ABSTRACT

This study investigates the issue of adaptive fault-tolerant neural control in strict-feedback nonlinear systems. The system is subjected to actuator faults, dead-zone and saturation. To model the unknown functions, radial basis function neural networks (RBFNN) are employed. The proposed approach utilizes a backstepping technique to formulate an adaptive fault-tolerant controller, drawing upon the Lyapunov stability theory and the approximation capabilities of RBFNN. The resultant controller guarantees the boundedness of all signals in the closed-loop system, ensuring precise tracking of the reference signal by the system output with a small, bounded error. Finally, simulation results are provided to illustrate the efficacy of the proposed strategy in addressing actuator faults, dead-zone, and saturation.

1. Introduction

Since there are many nonlinear systems in practical engineering, it has become a major problem to properly control the nonlinear systems [1]. Nonlinear systems possess a more intricate structure, presenting a greater challenge in designing controllers compared to the well-established theories and control methods applicable to linear systems [2]. The backstepping approach has evolved into a crucial tool to handle many kinds of nonlinear systems. However, this method necessitates that the system structure conforms to strict feedback requirements. It has been possible to get around the challenge in non-strict-feedback architectures by using the backstepping technique [3]. A great deal of effort has been put into developing approximation-based adaptive fuzzy or neural control for nonlinear systems in recent years [4,5]. In the pursuit of control design for nonlinear systems, the utilization of neural networks (NNs) or fuzzy logical systems (FLSs) is common for modeling unknown nonlinear functions, owing to their inherent ability in approximating functions [6,7]. Addressing a category of nonlinear systems characterized by unknown system functions, a proposed approach in the literature involves the application of adaptive fuzzy control [8]. Further adaptive fuzzy control techniques for nonlinear uncertain systems have been put forth [9]. On the other hand, by using RBFNN as function approximators, a number of adaptive control design approaches for nonlinear systems have been developed [10]. Through the use of a state observer, a fuzzy adaptive control problem for non-strict-feedback systems was taken into account and then expanded to include uncertain

* Corresponding author.
E-mail address: paolo.mercorelli@leuphana.de (P. Mercorelli).

https://doi.org/10.1016/j.jfranklin.2024.107471
Received 10 May 2024; Received in revised form 27 October 2024; Accepted 12 December 2024
Available online 17 December 2024

switching nonlinear systems [11]. Furthermore, a versatile controller was devised for systems with time delays in non-strict feedback configurations [12]. Additionally, in addressing nonlinear systems, a proposed method involves a non-strict-feedback adaptive sliding mode approach [13].

Actuator faults are frequently unavoidable in real-world control systems. They will contribute to system instability and potentially catastrophic accidents if they are ignored [14–16]. The control of systems with failed actuators has received increased attention as safety and reliability standards have risen [17–19]. It is essential and important to look at the issue of tolerance for faults in order to ensure system dependability and achieve the required control performance. Various FTC design methodologies have been introduced in the literature recently to tackle actuator faults in nonlinear systems [20–22]. For instance, an adaptive compensating control strategy has been demonstrated to be effective in addressing nonlinear systems afflicted with an infinite number of unknown actuator faults [23]. Additionally, an adaptive fuzzy output feedback fault-tolerant optimum controller has been developed for nonlinear systems in strict-feedback form [24]. A proposed approach in the literature for nonlinear systems with unmodeled dynamics and time-varying delays involves a fuzzy adaptive output-feedback tracking FTC methodology [25]. Furthermore, a specific class of nonlinear systems susceptible to actuation failures has been the focus of an adaptive finite-time tracking controller based on FLSs and the backstepping approach [26].

Non-smooth nonlinearities like dead-zone and saturation often arise in output gearbox devices, negatively impacting system performance and stability [27–29]. A dead zone in the actuator can degrade tracking performance and even lead to instability. To address this, two main approaches are used. One involves constructing an inverse of the dead-zone model, while the other converts it into a nonlinear function model, which simplifies control [30,31]. For example, adaptive fuzzy control for stochastic nonlinear systems with dead-zone has been studied [32], as well as adaptive inverse methods for unknown dead-zones [33,34]. Additionally, adaptive control for systems with time-varying state constraints and dead-zone via output feedback has been reported in [35].

Input saturation is a common limitation in industrial control systems that can degrade performance or even cause instability in closed-loop systems [36–38]. Addressing saturation nonlinearity has been a significant challenge, leading to notable advancements in recent years [39–41]. For instance, an adaptive fuzzy control method using enhanced command-filtered backstepping has been developed for MIMO nonlinear systems with input saturation [42]. Similarly, adaptive prescribed performance control and adaptive control for switched uncertain nonlinear systems with input saturation have been explored [43,44]. Additionally, a scheme for nonlinear systems with both input saturation and time delay has been proposed [45]. Most of the previously mentioned methods considered either dead-zone or saturation effects individually. However, some recent studies have addressed both dead-zone and saturation simultaneously. For instance, an adaptive command filter-based fuzzy control scheme has been developed for nonlinear systems with both dead-zone and saturation [46]. Additionally, an observer-based control method has been proposed for systems experiencing these non-linearities [47]. Similarly, a neural network-based output-feedback control approach has been designed for nonlinear systems under both saturation and dead-zone conditions [48]. Non-smooth nonlinearities like dead-zone and saturation can significantly degrade system performance and stability. Ignoring actuator faults can lead to catastrophic failures, emphasizing the necessity of considering these factors together to enhance safety and reliability. This motivated us to conduct this research, addressing actuator faults, dead-zone, and saturation simultaneously for strict-feedback nonlinear systems.

Based on the aforementioned results, this study addresses the challenge of adaptive fault-tolerant tracking control for nonlinear systems affected by actuator faults, dead-zones, and saturation. The following outlines the key contributions of this paper:

- Compared to existing results [15,20,21,29–31], this paper examines an adaptive neural fault-tolerant control problem for a class of strict-feedback nonlinear systems with actuator faults and input nonlinearities subjected to dead-zone and saturation. Unlike previous studies on actuator faults [14], which considered constant gain faults, this paper addresses time-varying gain faults and unknown bias faults, making the controller design more challenging. The approximation of unknown functions is achieved through radial basis function neural networks (RBFNNs). In comparison to fuzzy logic systems [10,11], RBFNNs offer advantages such as straightforward design, superior generalization capabilities, and the ability to linearize parameters.
- Compared to existing research on nonlinear systems that addresses either input dead-zone [33,34] or input saturation [37,38], the system considered in this paper incorporates both dead-zone and saturation, posing a significant challenge for controller design. The nonsmooth characteristics of input dead-zones and saturations are approximated by smooth affine functions with minimal approximation error, as justified by the mean-value theorem. As a result, the proposed control scheme is envisioned to be more applicable and effective in practical real-world applications.
- The Lyapunov stability theory and backstepping technique are employed in designing the adaptive neural fault-tolerant controller, ensuring that all signals in the closed-loop system exhibit bounded behavior. Additionally, the controller is designed to keep the tracking error within a bounded set.

The remaining portions of the paper are structured in the following manner: Section 2 furnishes a depiction of the problem formulation and outlines preliminaries. Following that, Section 3 presents the stability analysis and delineates the design scheme for the adaptive controller. Moving on to Section 4, a simulation example is scrutinized. Finally, Section 5 encapsulates the conclusion of this paper.

Notations. In this paper, the following notations are utilized consistently: $\mathbb{R}$ signifies the set of real numbers; $\mathbb{R}^n$ signifies the n-dimensional real space; y represents the system output, u is the system input, υ denotes the actual control law; $\bar{\zeta}_i = [\zeta_1, \zeta_2, \ldots, \zeta_i]^T \in \mathbb{R}^i$ for $i = 1, 2, \ldots, n$ represents the system state vector; $\|X\|$ signifies the Euclidean norm of a vector X.

2. Problem formulation and preliminaries

Consider the following nonlinear system in strict-feedback form as

$$\begin{cases} \dot{\zeta}_i &= \zeta_{i+1} + f_i(\bar{\zeta}_i), \quad 1 \le i \le n-1 \\ \dot{\zeta}_n &= u + f_n(\bar{\zeta}_n) \\ y &= \zeta_1 \end{cases} \tag{1}$$

where $\bar{\zeta}_i = [\zeta_1, \zeta_2, \dots, \zeta_i]^T \in \mathbb{R}^i$ for $i = 1, 2, \dots, n$ is the system state vector, ζ_i the denotes the ith component of the system state vector, $u \in \mathbb{R}$, and $y \in \mathbb{R}$ are the system input and system output, respectively. $f_i(\cdot) : \mathbb{R}^i \to \mathbb{R}$ is an unknown smooth function with $f_i(0) = 0$.

Actuator faults, involving input dead-zone and saturation need to be addressed in real-world situations due to the external environment's uncertainties, prolonged system operation, and the transmission mechanism's physical limitations.

The model representing actuator faults is defined as follows:

$$u = \rho(t, t_\rho)\chi(v) + u_r(t, t_r) \tag{2}$$

where $\rho(t, t_\rho) \in [0, 1]$ denotes the unknown time-varying fault, and $\chi(v)$ characterizes the input subjected to both dead-zone and saturation nonlinearity, with v serving as the control signal to be formulated. Moreover, the term $u_r(t, t_r)$ denotes the additive bias fault. The variable t_ρ marks the moment when the actuator loses its effectiveness, while t_r denotes the duration from the normal operating state to the occurrence of the first subsequent failure. At the common time t_0 for both t_r and t_ρ, the model describing actuator fault (2) is articulated as follows

$$u = \begin{cases} v & \text{if } t < t_0 \\ \rho(t, t_0)\chi(v) + u_r(t, t_0) & \text{if } t \ge t_0 \end{cases} \tag{3}$$

For $t < t_0$, the fault model simplifies to $u = v$, indicating normal actuation and for $t \ge t_0$, the actuator fault occurs.

Additionally, $\chi(v)$ is defined as follows:

$$\chi(v) = \begin{cases} R_N, & v < a_{s1} \\ t_s(v), & a_{s1} \le v < a_{s0} \\ 0, & a_{s0} < v \le b_{r0} \\ t_r(v), & a_{r0} < v \le a_{r1} \\ R_P, & v > a_{r1} \end{cases} \tag{4}$$

where $t_s(v)$ and $t_r(v)$ describe uncertain smooth functions. $R_N < 0$ and $R_P > 0$ represent the saturation parameters, and $a_{s1} < a_{s0} < 0$ and $0 < a_{r0} < a_{r1}$ represent the parameters of unknown input nonlinearity.

Remark 1. Compared to existing work [14], which proposes adaptive control schemes for a class of nonlinear systems including faults and quantization in the actuator, this study extends its scope to incorporate dead-zone and saturation effects in addition to actuator faults. Furthermore, while work [20] addresses dead-zone in the output mechanism, our study focuses on utilizing dead-zone and saturation effects specifically in the input of the system. In contrast to [20], which utilizes multi-dimensional Taylor networks for approximation, our approach employs radial basis function neural networks. Moreover, in comparison to works [21,22] where control schemes are proposed for nonlinear systems with dead-zone, this study uniquely considers the combined impact of dead-zone and saturation. Additionally, while work [22] is based on switched nonlinear systems, our proposed methodology is for non-switched systems. This control strategy proposed in this work not only addresses the complexities of non-switched systems but also remains applicable to switched systems, demonstrating its versatility across different system configurations.

Remark 2. Combining input dead-zone, saturation, and actuator faults together presents several difficulties. Determining the appropriate design parameters and initial conditions for the controller poses a challenge, as they often need to be refined through trial and error, a process that can consume significant time. The simultaneous consideration of dead-zone, saturation, and actuator faults complicates the controller design process, as each factor can interact and exacerbate the others. Ensuring the stability and performance of the system under the combined effect of these nonlinearities and faults is difficult and requires efficient control strategies and the selection of the right design parameters.

Control objective. This paper seeks to create an adaptive fault-tolerant controller with the following objectives:

(i) Ensure that the tracking error $e_1 = y - y_d$ converges to a small bounded set.
(ii) Maintain the boundedness of all signals within the closed-loop system.

Assumption 1 (*[1]*)**.** The reference signal y_d and its derivatives are continuous and bounded.

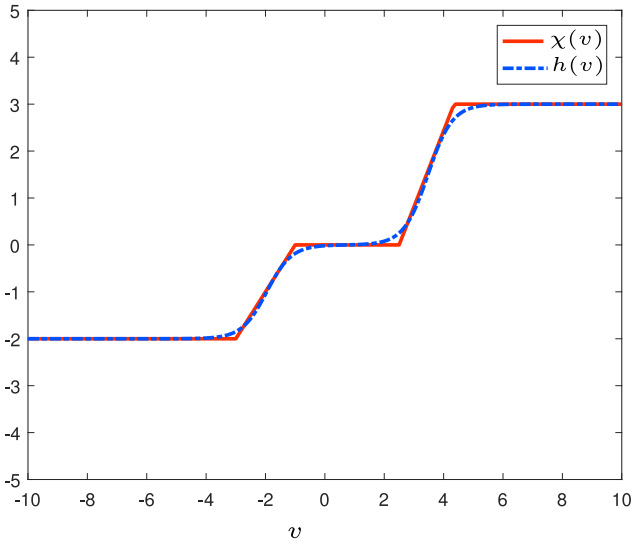

Fig. 1. The trajectories of $\chi(\upsilon)$ and $h(\upsilon)$.

Assumption 2 (*[46]*)**.** There exist unknown positive parameters a_{sl}, a_{rl}, a_{su}, and a_{ru} such that

$$0 < a_{sl} < t_s'(\upsilon) < a_{su} < \infty, \quad \forall \upsilon \in [a_{sl}, a_{s0}] \tag{5}$$

$$0 < a_{rl} < t_r'(\upsilon) < a_{ru} < \infty, \quad \forall \upsilon \in [a_{r1}, a_{r0}] \tag{6}$$

where $t_s'(\upsilon)$ and $t_r'(\upsilon)$ are the derivatives of $t_s(\upsilon)$ and $t_r(\upsilon)$.

Based on (4), it is evident that the dead zone and saturation may not necessarily be differentiable for any given υ. From the existing work [46], we can utilize the following smooth function to approximate it.

$$\begin{aligned} h(\upsilon) = & -\frac{R_N}{2}\tanh l_1\left(\upsilon - \frac{a_{s0}}{l_1} + \tau_l\right) \\ & + \frac{R_P}{2}\tanh l_2\left(\upsilon - \frac{a_{r0}}{l_2} + \tau_r\right) \\ & - \frac{R_N}{2}\tanh\left(a_{s0} - \tau_l l_1\right) + \frac{R_P}{2}\tanh\left(a_{n0} + \tau_r l_2\right) \end{aligned} \tag{7}$$

where l_1, l_2, τ_l, and τ_r are positive parameters that can be adjusted to minimize the approximation error. The curves of $\chi(\upsilon)$ and $h(\upsilon)$ are depicted in Fig. 1. Furthermore, the function $\chi(\upsilon)$ can be expressed as

$$\chi(\upsilon) = h(\upsilon) + p(\upsilon) \tag{8}$$

where $p(\upsilon) = \chi(\upsilon) - h(\upsilon)$ represents the estimation error. It can be observed from [46] that $p(\upsilon)$ is bounded. Therefore, we make the following assumption:

Assumption 3 (*[46]*)**.** There exists an unknown positive constant $\bar{p}$ such that $|p(\upsilon)| \le \bar{p}$.

Additionally, based on the mean-value theorem, there is $\upsilon_u \in (\upsilon_0, \upsilon)$ such that

$$h(\upsilon) = h(\upsilon_0) + \dot{h}(\upsilon_u)(\upsilon - \upsilon_0) \tag{9}$$

holds. By choosing $\upsilon_0 = 0$, the expression for $h(\upsilon)$ takes the following form

$$h(\upsilon) = \dot{h}(\upsilon_u)\upsilon, \tag{10}$$

where $\dot{h}(\upsilon_u)$ is expressed as

$$\begin{aligned} \dot{h}(\upsilon_u) = & -\frac{R_N l_1}{2}\frac{1}{\cosh^2 l_1\left(\upsilon_u - \frac{a_{s0}}{l_1} + \tau_1\right)} \\ & + \frac{R_P l_2}{2}\frac{1}{\cosh^2 l_2\left(\upsilon_u - \frac{a_{r0}}{l_2} - \tau_r\right)} \end{aligned} \tag{11}$$

Additionally, a_{s1}, a_{s0}, a_{r0}, a_{r1}, R_N, and R_P are assumed to be bounded ($R_N < 0$, $R_P > 0$, $l_1 > 0$, $l_2 > 0$), ensuring that $\dot{h}(\upsilon_u)$ remains bounded below when υ is confined within a closed set. This leads to the following assumption.

Assumption 4 ([46]). The derivative of the smoothing function $h(\upsilon)$ can be expressed as follows:

$$0 < \omega_1 < \dot{h}(\upsilon_u) < \omega_2 \tag{12}$$

where ω_1 and ω_2 are unknown positive constants.

Assumption 5 ([14]). The time-varying gain fault $\rho(t,t_\rho)$ and the additive bias fault $u_r(t,t_r)$ exhibit bounded behavior. Specifically, there exists a positive constant $\rho_{\min}$ such that $\rho_{\min} < \rho(t,t_\rho) \leq 1$, and there exists another positive constant $u_{\max}$ such that $|u_r(t,t_r)| \leq u_{\max}$.

Remark 3. Assumption 1 is often employed in the tracking control of nonlinear systems to aid in the subsequent Lyapunov stability analysis. Assumptions 2, 3, and 4 are generally utilized to tackle issues related to input saturation and dead-zone, thereby simplifying the stability analysis process and these assumptions are well-documented in the literature [46–48]. According to Assumption 5, the time-varying control gain $\rho(t,t_\rho)$ and the additive bias fault $u_r(t,t_r)$ are considered unknown. This assumption helps to ease the stability criterion and is frequently observed in recent publications [15,20].

Remark 4. In (2), if $\rho(t,t_\rho) = 1$ and $u_r(t,t_r) = 0$, then $u = \chi(\upsilon)$. This indicates that the actuator is affected only by dead-zone and saturation. Conversely, if $\rho(t,t_\rho) \neq 1$ and $u_r(t,t_r) = 0$, it suggests a loss of effectiveness in the actuator. Additionally, other types of sensor faults may occur when $\rho(t,t_\rho) = 0$ and $u_r(t,t_r) \neq 0$. According to Assumption 5, we consider slow-varying faults with variations not exceeding 1. Furthermore, the additive fault $u_r(t,t_r)$ is bounded by the physical limits of the actuators and cannot be excessively large and both $\rho(t,t_\rho)$ and $u_r(t,t_r)$ are treated as unknowns. The unpredictable occurrence of time-varying actuator faults can degrade system performance and complicate controller design. In (3), the scenario involves an actuator fault occurring at a specific time t_0, which serves as a threshold time. To simplify the analysis and modeling, it is assumed that both $\rho(t,t_\rho)$ and $u_r(t,t_r)$ align at this threshold time t_0. Thus, $t_\rho = t_r = t_0$ is set in (3), aligning the timing of these fault parameters for clarity and consistency in the analysis.

Lemma 1 (*Young's Inequality* [49]). *For all* $(m,n) \in \mathbb{R}^2$, $\epsilon > 0$ *the following inequality holds:*

$$mn \leq \frac{\epsilon^p}{p}|m|^p + \frac{1}{q\epsilon^p}|n|^q, \tag{13}$$

where $p > 1$, $q > 1$, *and* $(p-1)(q-1) = 1$.

Lemma 2 ([50]). *For any positive, continuous function* $V(t)$ *defined for all* $t \in \mathbb{R}$ *and possessing a bounded initial condition, if the derivative* $\dot{V}(t) \leq -aV(t) + b$, *where* a *and* b *are positive constants, then the function* $V(t)$ *maintains boundedness.*

In this study, RBFNN [2] are used to approximate unknown functions. There are neural networks designated as $W^{*T}Q(Z)$ and a constant $\epsilon > 0$ such that the following approximation employs for any continuous smooth uncertain function $\bar{f}(Z)$ defined in a set $Z \in \mathbb{R}^q$, one has

$$\bar{f}(Z) = W^{*T}Q(Z) + \delta(Z), \quad |\delta(Z)| \leq \epsilon, \tag{14}$$

where $\delta(Z)$ represents the approximation error, and $W^* = [W_1^*, W_2^*, \ldots, W_N^*]^T$ denotes the ideal weight vector, which is defined as

$$W^* = \arg\min_{W \in \mathbb{R}^N} \left[\sup_{Z \in Z} \left| f(Z) - W^T Q(Z) \right| \right], \tag{15}$$

where $W = [W_1, W_2, \ldots, W_N]^T$ with N being the number of nodes in the neural networks. The vector $Q(Z) = [Q_1(Z), Q_2(Z), \ldots, Q_N(Z)]$ represents the basis functions, and each component $Q_i(Z)$ is defined as

$$Q_i(Z) = \exp\left(-\frac{(Z-\mu_i)^T(Z-\mu_i)}{v_i^2} \right), \quad i = 1,2,\ldots,N, \tag{16}$$

where μ_i and v_i represent the center and width of the Gaussian function, respectively.

3. Adaptive neural fault-tolerant controller design and stability analysis

In this section, the control strategy for the nonlinear system (1) is developed, utilizing the backstepping method and a neural network approximation. This approach is facilitated by the following coordinate transformation:

$$e_1 = \zeta_1 - y_d \tag{17}$$

$$e_i = \zeta_i - \alpha_{i-1}, \quad i = 2,\ldots,n \tag{18}$$

where α_{i-1} denotes the virtual controller to be developed.

Step 1. From (1) and $e_1 = \zeta_1 - y_d$, we have

$$\dot{e}_1 = \zeta_2 + f_1 - \dot{y}_d = e_2 + \alpha_1 + f_1 - \dot{y}_d. \tag{19}$$

Now, consider a Lyapunov function as

$$V_1 = \frac{1}{2}e_1^2 + \frac{1}{2b_1}\tilde{\theta}_1^2, \tag{20}$$

where $\tilde{\theta}_1 = \theta_1 - \hat{\theta}_1$ denotes the estimation with $\hat{\theta}_1$ being the estimated value of the unknown parameter θ_1, and $b_1 > 0$ serves as a design parameter.

Now, differentiate (20), one has

$$\begin{aligned}\dot{V}_1 &= e_1(e_2 + \alpha_1 + f_1 - \dot{y}_d) - \frac{1}{b_1}\tilde{\theta}_1\dot{\hat{\theta}}_1 \\ &= e_1\left(e_2 + \alpha_1 + \bar{f}_1(Z_1)\right) - \frac{1}{2}e_1^2 - \frac{1}{b_1}\tilde{\theta}_1\dot{\hat{\theta}}_1,\end{aligned} \tag{21}$$

where $\bar{f}_1(Z_1) = f_1 - \dot{y}_d + \frac{1}{2}e_1$.

Since $\bar{f}_1(Z_1)$ encompasses an unknown nonlinear function f_1, addressing this challenge can be accomplished by using RBFNN to approximate the unknown function $\bar{f}_1(Z_1)$. For any $\epsilon_1 > 0$, the following holds

$$\bar{f}_1(Z_1) = W_1^T Q_1(Z_1) + \delta_1(Z_1), \quad |\delta_1(Z_1)| \le \epsilon_1. \tag{22}$$

With the help completion squares, one has

$$\begin{aligned}e_1\bar{f}_1(Z_1) &= e_1\left(W_1^{*T}Q_1(Z_1) + \delta_1(Z_1)\right) \\ &\le |e_1|\left(\|W_1^*\|\|Q_1(Z_1)\| + \epsilon_1\right) \\ &\le |e_1|\left(\|W_1^*\|\|Q_1(Z_1)\| + \epsilon_1\right) \\ &\le \frac{1}{2\beta_1^2}e_1^2\theta_1 Q_1^T(Z_1)Q_1(Z_1) + \frac{\beta_1^2}{2} + \frac{e_1^2}{2} + \frac{\epsilon_1^2}{2},\end{aligned} \tag{23}$$

where $\beta_1 > 0$ is a design parameter, $\theta_1 = \|W_1^*\|^2$, and $Z_1 = [\zeta_1, y_d, \dot{y}_d]^T$.

Design the virtual controller α_1 as

$$\alpha_1 = -k_1 e_1 - \frac{1}{2\beta_1^2}e_1\hat{\theta}_1 Q_1^T(Z_1)Q_1(Z_1), \tag{24}$$

where $k_1 > 0$ and $\beta_1 > 0$ represent design parameters.

By employing Lemma 1 and (24), we have

$$e_1\alpha_1 \le -k_1 e_1^2 - \frac{1}{2\beta_1^2}e_1^2\hat{\theta}_1 Q_1^T(Z_1)Q_1(Z_1). \tag{25}$$

By using (25) and (23) into (21), we have

$$\dot{V}_1 \le -k_1 e_1^2 + \left(\frac{1}{2\beta_1^2}e_1^2 Q_1^T(Z_1)Q_1(Z_1)\right)(\theta_1 - \hat{\theta}_1) + \frac{\beta_1^2}{2} + \frac{e_1^2}{2} + \frac{\epsilon_1^2}{2} \tag{26}$$

Since $\tilde{\theta}_1 = \theta_1 - \hat{\theta}_1$, becomes

$$\dot{V}_1 \le -k_1 e_1^2 + \frac{1}{b_1}\tilde{\theta}_1\left(\frac{1}{2\beta_1^2}b_1 e_1^2\hat{\theta}_1 Q_1^T(Z_1)Q_1(Z_1) - \dot{\hat{\theta}}_1\right) + \frac{\beta_1^2}{2} + \frac{e_1^2}{2} + \frac{\epsilon_1^2}{2}. \tag{27}$$

The adaptation law $\hat{\theta}_1$ can be defined as

$$\dot{\hat{\theta}}_1 = \frac{b_1}{2\beta_1^2}e_2^2 Q_1^T(Z_1)Q_1(Z_1) - \varrho_1\hat{\theta}_1, \tag{28}$$

where $b_1 > 0$, $\varrho_1 > 0$, and $\beta_1 > 0$ represent the design parameters. Substituting (28) into (27), we have

$$\dot{V}_1 \le -k_1 e_1^2 + e_1 e_2 + \frac{\varrho_1}{\beta_1}\tilde{\theta}_1\hat{\theta}_1 + \frac{1}{2}\beta_1^2 + \frac{1}{2}\epsilon_1^2. \tag{29}$$

Step i. $(2 \le i \le n-1)$. From (1) and (18), we have

$$\dot{e}_i = e_{i+1} + \alpha_i + f_i - \dot{\alpha}_{i-1} \tag{30}$$

Take the Lyapunov function as

$$V_i = V_{i-1} + \frac{1}{2}e_i^2 + \frac{1}{2b_i}\tilde{\theta}_i^2, \tag{31}$$

where $\tilde{\theta}_i = \theta_i - \hat{\theta}_i$ denotes the estimation with $\hat{\theta}_i$ being the estimated value of the unknown parameter θ_i, and $b_i > 0$ serves as a design parameter.

By differentiating (28), one has

$$\begin{aligned}\dot{V}_i \le & -\sum_{j=1}^{i-1} k_j e_j^2 + e_{i-1}e_i + \sum_{j=1}^{i-1}\frac{\varrho_j}{b_j}\tilde{\theta}_j\hat{\theta}_j + \sum_{j=1}^{i-1}\frac{\beta_j^2}{2} + \frac{\epsilon_j^2}{2} \\ & + e_i(e_{i+1} + \alpha_i + \bar{f}_i(Z_i)) - \frac{1}{2}e_i^2 - -\frac{1}{b_i}\tilde{\theta}_i\dot{\hat{\theta}}_i,\end{aligned} \tag{32}$$

where

$$\bar{f}_i(Z_i) = e_{i-1} + f_i - \dot{\alpha}_{i-1} + \frac{1}{2}e_i. \tag{33}$$

Since $\bar{f}_i(Z_i)$ encompasses an unknown nonlinear function f_i, addressing this challenge can be accomplished by using RBFNN to approximate the unknown function $\bar{f}_i(Z_i)$. For every $\epsilon_i > 0$, the following holds

$$\bar{f}_i(Z_i) = W_i^T Q_i(Z_i) + \delta_i(Z_i), \quad |\delta_i(Z_i)| \le \epsilon_i. \tag{34}$$

By taking the same method as (23), one has

$$e_i\bar{f}_i(Z_i) \le \frac{1}{2\beta_i^2}e_i^2\theta_i Q_i^T(Z_i)Q_i(Z_i) + \frac{\beta_i^2}{2} + \frac{e_i^2}{2} + \frac{\epsilon_i^2}{2}, \tag{35}$$

where $\theta_i = \|W_i^*\|^2$, $Z_i = [\zeta_1, \ldots, \zeta_i, \hat{\theta}_1, \ldots, \hat{\theta}_{i-1}, y_d, \ldots, y_d^{(i)}]^T$, and β_i being a positive design parameter.

Define the virtual control law α_i as

$$\alpha_i = -k_i e_i - \frac{1}{2\beta_i^2}e_i\hat{\theta}_i Q_i^T(Z_i)Q_i(Z_i), \tag{36}$$

where $k_i > 0$ and $\beta_i > 0$ represent the design parameters.

By employing Lemma 1 and (2), we have

$$e_1\alpha_i \le -k_i e_i^2 - \frac{1}{2\beta_i^2}e_i^2\hat{\theta}_i Q_i^T(Z_i)Q_i(Z_i). \tag{37}$$

By using (35) and (37) into (32), we have

$$\begin{aligned}\dot{V}_i \le & -\sum_{j=1}^{i-1} k_j e_j^2 + e_{i-1}e_i + \sum_{j=1}^{i-1}\frac{\varrho_j}{b_j}\tilde{\theta}_j\hat{\theta}_j + \sum_{j=1}^{i}\left(\frac{\beta_j^2}{2} + \frac{\epsilon_j^2}{2}\right) \\ & + \left(\frac{1}{2\beta_i^2}e_i^2 Q_i^T(Z_i)Q_i(Z_i)\right)(\theta_i - \hat{\theta}_i) - \frac{1}{b_i}\tilde{\theta}_i\dot{\hat{\theta}}_i\end{aligned} \tag{38}$$

Since $\tilde{\theta}_i = \theta_i - \hat{\theta}_i$, (38) becomes

$$\begin{aligned}\dot{V}_i \le & -\sum_{j=1}^{i-1} k_j e_j^2 + e_{i-1}e_i + \sum_{j=1}^{i-1}\frac{\varrho_j}{b_j}\tilde{\theta}_j\hat{\theta}_j + \sum_{j=1}^{i}\left(\frac{\beta_j^2}{2} + \frac{\epsilon_j^2}{2}\right) \\ & + \frac{1}{b_i}\tilde{\theta}_i\left(\frac{1}{2\beta_i^2}b_i e_i^2 Q_i^T(Z_i)Q_i(Z_i) - \dot{\hat{\theta}}_i\right).\end{aligned} \tag{39}$$

The adaptation law $\hat{\theta}_i$ can be define as

$$\dot{\hat{\theta}}_i = \frac{b_i}{2\beta_i^2}e_i^2 Q_i^T(Z_i)Q_i(Z_i) - \varrho_i\hat{\theta}_i, \tag{40}$$

with $b_i > 0$, $\varrho_i > 0$, and $\beta_i > 0$ being the design parameters.

Substituting (40) into (39), one has

$$\dot{V}_i \le -\sum_{j=1}^{i} k_i e_j^2 + e_i e_{i+1} + \sum_{j=1}^{i}\frac{\varrho_j}{\beta_j}\tilde{\theta}_j\hat{\theta}_j + \sum_{j=1}^{i}\left(\frac{\beta_j^2}{2} + \frac{\epsilon_j^2}{2}\right). \tag{41}$$

Step n. By employing (1), (2), (8), and (18), and calculating the time derivative of e_n, one has

$$\begin{aligned}\dot{e}_n &= u + f_n - \dot{\alpha}_{n-1} \\ &= (\rho(t,t_\rho)h(v) + \rho(t,t_\rho)p(v) + u_r(t,t_r)) + f_n - \dot{\alpha}_{n-1}.\end{aligned} \tag{42}$$

Consider the following Lyapunov function as

$$V_n = V_{n-1} + \frac{1}{2}e_n^2 + \frac{\omega_1}{2b_n}\tilde{\theta}_n^2, \tag{43}$$

where $\tilde{\theta}_n = \theta_n - \hat{\theta}_n$ denotes the estimation with $\hat{\theta}_n$ being the estimated value of the unknown parameter θ_n, and $b_n > 0$ serves as a design parameter.

Differentiating (37) yields

$$\begin{aligned}\dot{V}_n \le & -\sum_{j=1}^{n-1} k_j e_j^2 + e_{n-1}e_n + \sum_{j=1}^{n-1}\frac{\varrho_j}{b_j}\tilde{\theta}_j\hat{\theta}_j + \sum_{j=1}^{n-1}\frac{\beta_j^2}{2} + \frac{\epsilon_j^2}{2} \\ & + e_n\left((\rho(t,t_\rho)h(\upsilon) + \rho(t,t_\rho)p(\upsilon) + u_r(t,t_r)) + f_n(Z_n)\right) \\ & - \frac{1}{2}e_n^2 - \frac{\omega_1}{b_n}\tilde{\theta}_n\dot{\hat{\theta}}_n,\end{aligned} \tag{44}$$

where

$$\bar{f}_n(Z_n) = e_{n-1} + f_n - \dot{\alpha}_{n-1} + \frac{1}{2}e_n. \tag{45}$$

Since $\bar{f}_n(Z_n)$ encompasses an unknown nonlinear function f_n, addressing this challenge can be accomplished by using RBFNN to approximate the unknown function $\bar{f}_n(Z_n)$. For every $\epsilon_n > 0$, the following holds

$$\bar{f}_n(Z_n) = W_n^T Q_n(Z_n) + \delta_n(Z_n), \quad |\delta_n(Z_n)| \le \epsilon_n. \tag{46}$$

Similar to (32), one has

$$e_n\bar{f}(Z_n) \le \frac{\omega_1}{2\beta_n^2}e_n^2\theta_n Q_n^T(Z_n)Q_n(Z_n) + \frac{\beta_n^2}{2} + \frac{e_n^2}{2} + \frac{\epsilon_n^2}{2}, \tag{47}$$

where $\theta_n = \|W_n^*\|^2$, $Z_n = [\zeta_1, \ldots, \zeta_n, \hat{\theta}_1, \ldots, \hat{\theta}_{n-1}, y_d, \ldots, y_d^{(n)}]^T$, and β_n being a positive design parameter.

Define the real control law υ as

$$\upsilon = -k_n e_n - \frac{1}{2\beta_n^2\rho_{\min}}e_n\hat{\theta}_n Q_n^T(Z_n)Q_n(Z_n). \tag{48}$$

Based on Lemma 1 and Assumption 5, we have

$$e_n u_r(t,t_r) \le \frac{1}{2}e_n^2 + \frac{1}{2}u_{\max}^2. \tag{49}$$

From Assumptions 3–5, Lemma 1, (10), and (48), one has

$$\rho(t,t_\rho)h(\upsilon) \le -k_n\rho_{\min}\omega_1 e_n^2 - \frac{\omega_1}{2\beta_n^2}e_n^2\hat{\theta}_n Q_n^T(Z_n)Q_n(Z_n), \tag{50}$$

$$\rho(t,t_\rho)p(\upsilon) \le \frac{1}{2}e_n^2 + \frac{1}{2}\bar{p}^2\rho_{\min}^2. \tag{51}$$

By using (47)–(51) into (44), one has

$$\begin{aligned}\dot{V}_n \le & -\sum_{j=1}^{n-1} k_j e_j^2 - k_n\rho_{\min}\omega_1 e_n^2 + \sum_{j=1}^{n}\frac{\varrho_j}{b_j}\tilde{\theta}_j\hat{\theta}_j + \sum_{j=1}^{n}\left(\frac{\beta_j^2}{2} + \frac{\epsilon_j^2}{2}\right) \\ & + \left(\frac{\omega_1}{2\beta_n^2}e_n^2 Q_n^T(Z_n)Q_n(Z_n)\right)(\theta_n - \hat{\theta}_n) - \frac{\omega_1}{b_n}\tilde{\theta}_n\dot{\hat{\theta}}_n + \frac{1}{2}u_{\max}^2 + \frac{1}{2}\bar{p}^2\rho_{\min}^2\end{aligned} \tag{52}$$

Since $\tilde{\theta}_n = \theta_n - \hat{\theta}_n$, (52) becomes

$$\begin{aligned}\dot{V}_n \le & -\sum_{j=1}^{n-1} k_j e_j^2 - k_n\rho_{\min}\omega_1 e_n^2 + \sum_{j=1}^{n}\frac{\varrho_j}{b_j}\tilde{\theta}_j\hat{\theta}_j + \sum_{j=1}^{n}\left(\frac{\beta_j^2}{2} + \frac{\epsilon_j^2}{2}\right) \\ & + \frac{\omega_1}{b_n}\tilde{\theta}_n\left(\frac{1}{2\beta_n^2}e_n^2 Q_n^T(Z_n)Q_n(Z_n) - \dot{\hat{\theta}}_n\right) + \frac{1}{2}u_{\max}^2 + \frac{1}{2}\bar{p}^2\rho_{\min}^2\end{aligned} \tag{53}$$

The adaptation law $\hat{\theta}_n$ can be defined as

$$\dot{\hat{\theta}}_n = \frac{b_n}{2\beta_n^2}e_n^2 Q_n^T(Z_n)Q_n(Z_n) - \varrho_n\theta_n, \tag{54}$$

with k_n and ϱ_n being the positive design parameters.

By employing (54) into (53), one has

$$\begin{aligned}\dot{V}_n \le & -\sum_{j=1}^{n-1} k_n e_j^2 - k_n\rho_{\min}\omega_1 e_n^2 + \sum_{j=1}^{n-1}\frac{\varrho_j}{b_j}\tilde{\theta}_j\hat{\theta}_j + \frac{\varrho_n\omega_1}{b_n}\tilde{\theta}_n\hat{\theta}_n \\ & + \sum_{j=1}^{n}\left(\frac{\beta_j^2}{2} + \frac{\epsilon_j^2}{2}\right) + \frac{1}{2}u_{\max}^2 + \frac{1}{2}\bar{p}^2\rho_{\min}^2.\end{aligned} \tag{55}$$

The control system's block representation is illustrated in Fig. 2.

Theorem 1. *For system (1) with actuator faults, saturation, and dead-zones, under Assumptions 1–5, the proposed control approach incorporates virtual controllers (24) and (36), a real controller (48), and adaptive laws (28), (40), and (54). This approach ensures that the tracking error $e_1 = y - y_d$ converges to a small bounded set, and achieves boundedness of all signals within the closed-loop system.*

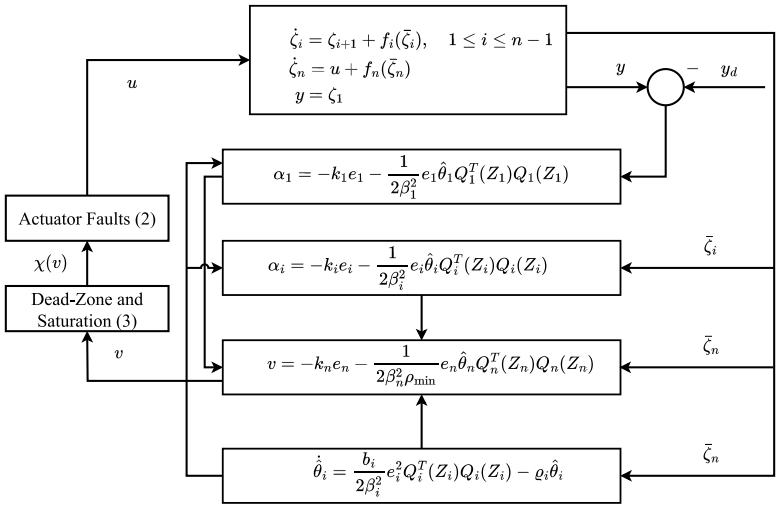

Fig. 2. Block representation of control system.

Proof. According to Lemma 1, we have

$$\tilde{\theta}_i \hat{\theta}_i \le -\frac{1}{2}\tilde{\theta}_i^2 + \frac{1}{2}\theta_i^2. \tag{56}$$

Combining (56) and (55), one has

$$\begin{aligned} \dot{V}_n \le & -\sum_{j=1}^{n-1} k_n e_j^2 - k_n \rho_{\min} \omega_1 e_n^2 + \sum_{j=1}^{n} \left(\frac{\beta_j^2}{2} + \frac{\epsilon_j^2}{2} \right) \\ & + \frac{1}{2} u_{\max}^2 + \frac{1}{2} \bar{p}^2 \rho_{\min}^2 - \sum_{i=1}^{n-1} \frac{\varrho_j}{2\beta_j} \tilde{\theta}_j^2 + \sum_{i=1}^{n-1} \frac{\varrho_j}{2\beta_j} \theta_j^2 - \frac{\varrho_n \omega_1}{2\beta_n} \tilde{\theta}_n^2 + \frac{\varrho_n \omega_1}{2\beta_n} \theta_n^2 \\ & \le -aV_n + b, \end{aligned} \tag{57}$$

where $a = \min\{2k_i, \ldots, 2k_{n-1}, 2k_n\omega_1\rho_{\min}, \beta_1, \ldots, \beta_n\}$, and $b = \sum_{j=1}^{n} \left(\frac{\beta_j^2}{2} + \frac{\epsilon_j^2}{2} \right) + \frac{1}{2} u_{\max}^2 + \frac{1}{2} \bar{p}^2 \rho_{\min}^2 + \sum_{i=1}^{n-1} \frac{\varrho_j}{2\beta_j} \theta_j^2 + \frac{\varrho_n \omega_1}{2\beta_n} \theta_n^2$.

Multiply both sides of (57) by e^{at}, one has

$$\frac{d(V_n e^{at})}{dt} \le b e^{-at}, \tag{58}$$

Integrating over the interval $[0, t]$ yields

$$V_n(t) \le \left(V_n(0) - \frac{b}{a} \right) e^{-at} + \frac{b}{a}, \tag{59}$$

which means that all signals stay bounded in the closed-loop system.

From (43) and (59), we have

$$e_1^2 \le 2 \left(V_n(0) - \frac{b}{a} \right) e^{-at} + \frac{b}{a}. \tag{60}$$

By taking the limits of (60), one has

$$\lim_{t \to \infty} |e_1| = \lim_{t \to \infty} |y - y_d| \le \sqrt{\frac{b}{a}}. \tag{61}$$

The proof is thus completed. □

Remark 5. The effectiveness of the control system heavily depends on the selection of controller parameters k_i, ϱ_i, and β_i. Enhancing the design parameters k_i and ϱ_i while minimizing β_i can significantly enhance system performance. Nevertheless, increasing k_i values may result in larger control signal magnitudes. Hence, achieving desirable control performance necessitates meticulous adjustment and optimization of these design parameters.

Remark 6. Compared to fuzzy logic systems [51], RBFNNs offer advantages such as straightforward design, superior generalization capabilities, and the ability to linearize parameters. Depending on the problem's nature and the desired results, each technique offers

unique features that make it suitable for a particular application. Furthermore, our work extends this comparison by addressing the practical challenges posed by simultaneous actuation effectiveness and uncontrollable additive actuation faults, an aspect not typically explored in existing fault-tolerant control studies. In contrast to studies focusing on linear sensor faults [52] and state estimation through observers [53], our approach assumes all states are directly measurable, enhancing the applicability of our proposed methodology in real-world scenarios.

4. Simulation results

Two examples are given in this section to demonstrate the efficacy of the suggested method.

Example 1. Consider the following strict-feedback nonlinear system as

$$\begin{cases} \dot{\zeta}_1 = f_1(\zeta_1) + \zeta_2 \\ \dot{\zeta}_2 = f_2(\zeta_1, \zeta_2) + u \\ y = \zeta_1 \end{cases} \tag{62}$$

where $f_1(\zeta_1) = \zeta_1 e^{-0.5\zeta_1}$ and $f_2(\zeta_1, \zeta_2) = \zeta_1 \sin(\zeta_2^2)$. The given tracking reference signal is $y_r = \frac{1}{2}\sin(t)$.

The description of the actuator fault model is as follows:

$$u = \begin{cases} \upsilon & \text{if } t < 10 \\ 0.2 + 0.8e^{-0.2t}\chi(\upsilon) + (\cos(\zeta_1))^2\zeta_2 & \text{if } t \geq 10 \end{cases} \tag{63}$$

where $\rho(t, t_\rho) = 0.2 + 0.8e^{-0.2t}$, $u_r(t, t_r) = (\cos(\zeta_1))^2\zeta_2$, $t_0 = 10$ is the common time for both t_r and t_ρ. For $t < 10$, the fault model simplifies to $u = \upsilon$, indicating normal actuation and for $t \geq 10$, the actuator fault occurs.

The input $\chi(\upsilon)$ subjected to dead-zone and saturation is defined as

$$\chi(\upsilon) = \begin{cases} -5 & \text{if } \upsilon \leq -5 \\ \frac{5}{4.5}(\upsilon + 0.5) & \text{if } -5 < \upsilon \leq -0.5 \\ 0 & \text{if } -0.5 < \upsilon \leq 0.5 \\ \frac{5}{4.5}(\upsilon - 0.5) & \text{if } 0.5 < \upsilon \leq 5 \\ 5 & \text{if } \upsilon > 5 \end{cases} \tag{64}$$

Based on Theorem 1, we determine the virtual control law α_i and the real control law υ as

$$\alpha_1 = -k_1 e_1 - \frac{1}{2\beta_1^2} e_1 \hat{\theta}_1 Q_1^T(Z_1) Q_1(Z_1), \tag{65}$$

$$\upsilon = -k_2 e_2 - \frac{1}{2\beta_2^2 \rho_{\min}} e_2 \hat{\theta}_2 Q_2^T(Z_2) Q_2(Z_2). \tag{66}$$

The adaptive law is chosen as

$$\dot{\hat{\theta}}_i = \frac{b_i}{2\beta_i^2} e_i^2 Q_i^T(Z_i) Q_i(Z_i) - \varrho_i \hat{\theta}_i, \quad i = 1, 2. \tag{67}$$

In the simulation, the initial conditions are chosen via rial-and-error method as $[\zeta_1(0), \zeta_2(0)]^T = [0.1, 0.1]^T$ and $[\hat{\theta}_1(0), \hat{\theta}_2(0)]^T = [0, 0]^T$. The design parameters, determined through a trial-and-error method, are $k_1 = 50, k_2 = 50$, $\beta_1 = 2, \beta_2 = 2$, $b_1 = 0.5, b_2 = 0.5$, $\varrho_1 = 0.05, \varrho_2 = 0.05$. The center and width of the RBFNN are also chosen through trial and error as $\mu_i = [-2, 2]$ and $\nu_i = 2$ for $i = 1, 2$.

Simulation results shown in Figs. 3 to 11 confirm the effectiveness of the closed-loop system. Fig. 3 displays both the system output y and the reference signal y_d. Fig. 4 illustrates the bounded tracking error e_1. Within Fig. 4, a zoomed-in view shows the impact of actuator faults for $t \geq 10$. Fig. 5 illustrates the bounded behavior of the state variable ζ_2. The bounded response curves of the adaptive parameters are shown in Fig. 6. Fig. 7 displays the plot of the control input υ, while Fig. 8 depicts the plot of the system input u. The combined plots of υ and u are shown in Fig. 9. Within Fig. 9, a zoomed-in view shows the impact of actuator faults for $t \geq 10$. Fig. 10 displays the input $\chi(\upsilon)$. To highlight the advantages of the proposed adaptive control scheme, we compared it with an existing control method [17]. Fig. 11 presents the comparative results based on the tracking error $e_1 = y - y_d$, demonstrating that the proposed method slightly outperforms the existing control method [17]. The simulation results confirm that all signals within the closed-loop system remain within defined bounds, demonstrating effective tracking performance.

To emphasize the benefits of the proposed adaptive control scheme, we compared it with an existing control method [17]. Three performance metrics as defined in [54], are utilized: the integral time absolute error (ITAE), defined as

$$\text{ITAE} = \int_0^T |e_1(t)|\, dt, \tag{68}$$

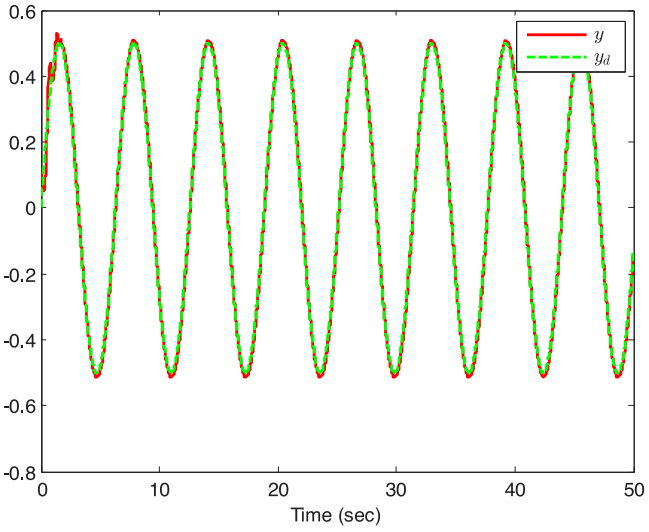

Fig. 3. Trajectories of y and y_d.

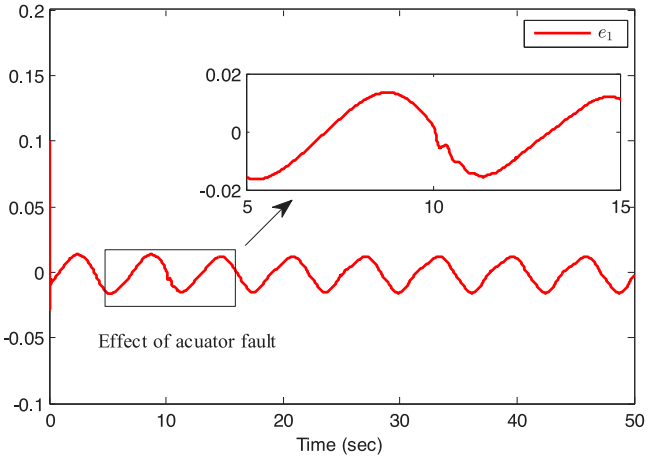

Fig. 4. The response of tracking error $e_1 = y - y_d$.

Table 1
Performance comparison of control methods.

Performance indices	Proposed method	Ref. [17]
ITAE	10.2873	13.5513
RMSE	0.0097	0.0124
MAE	0.0084	0.0108

the root-mean-square error (RMSE), calculated as

$$\text{RMSE} = \sqrt{\frac{1}{T}\int_0^T e_1^2(t)\,dt}, \tag{69}$$

and the mean absolute error (MAE), given by

$$\text{MAE} = \frac{1}{T}\int_0^T |e_1(t)|\,dt. \tag{70}$$

The results, summarized in Table 1, show that our proposed method consistently surpasses the existing control method [17], even in the presence of actuator faults, dead-zone, and saturation, which demonstrates the practicality of the proposed approach.

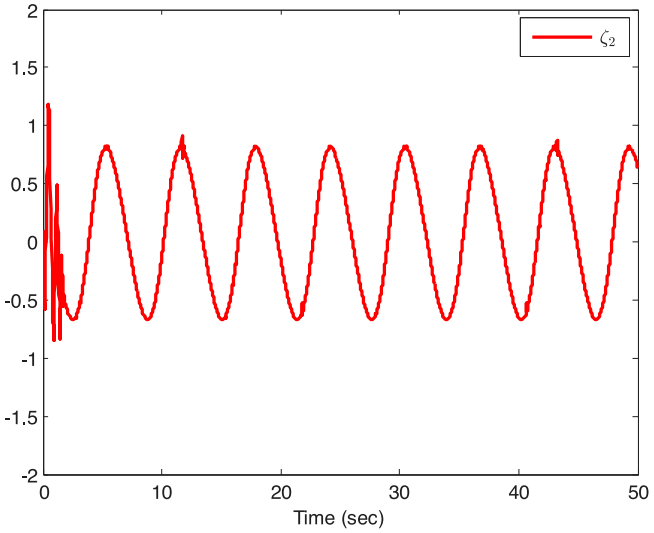

Fig. 5. The trajectories of state variable ζ_2.

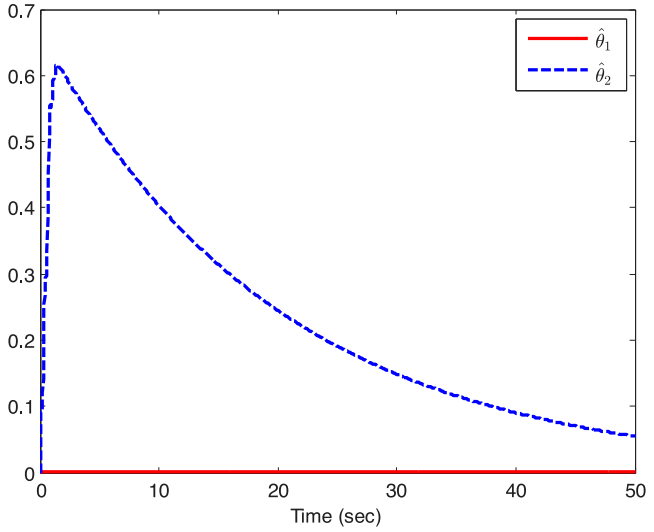

Fig. 6. The trajectories of adaptive laws.

Example 2. In this example the following one-link manipulator system as shown in Fig. 12 is used to show the accuracy of the proposed control method [55]

$$\begin{cases} D\ddot{q} + B\dot{q} + N\sin(q) = \tau \\ B_m\dot{\tau} + H\tau = V_0 - K\dot{q} \end{cases} \tag{71}$$

where q, $\dot{q}$, and $\ddot{q}$ represent the link position, velocity, and acceleration, respectively. $V_0 = u$ represents the input, and τ denotes the joint dynamic torque.

The meaning and values of the parameters of the manipulator are same as in [55].

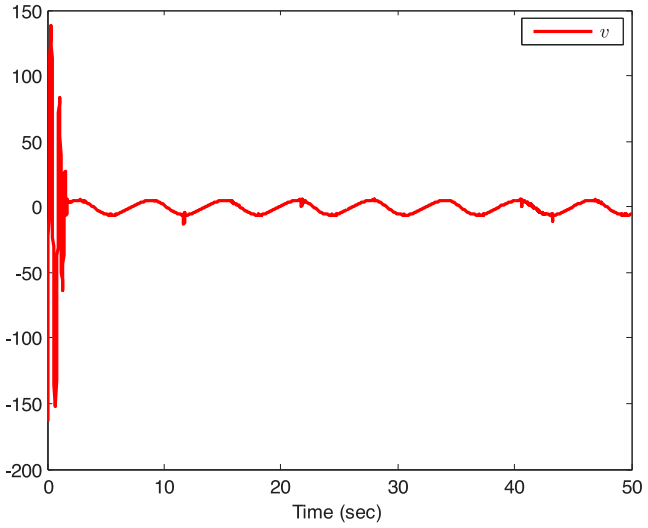

Fig. 7. The trajectory of control input v.

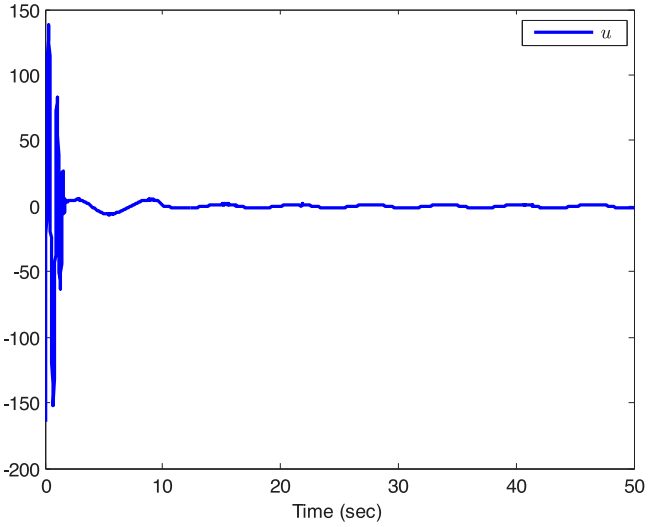

Fig. 8. The trajectory of system input u.

To simplify the system model, we introduce the variables as $\zeta_1 = q$, $\zeta_2 = \dot{q}$, $\zeta_3 = \tau$. The system dynamics described by (71) can be rewritten as

$$\begin{cases} \dot{\zeta}_1 = f_1(\zeta_1) + \zeta_2 \\ \dot{\zeta}_2 = f_2(\zeta_1, \zeta_2) + \frac{1}{D}\zeta_3 \\ \dot{\zeta}_3 = f_3(\zeta_1, \zeta_2, \zeta_3) + \frac{1}{M}u \\ y = \zeta_1 \end{cases} \tag{72}$$

where $f_1(\zeta_1) = 0$, $f_2(\zeta_1, \zeta_2) = \frac{1}{D}(-B\zeta_2 - N\sin(\zeta_1))$ and $f_3(\zeta_1, \zeta_2, \zeta_3) = \frac{1}{B_m}(-K\zeta_2 - H\zeta_3)$. The reference signal for this example is chosen as $y_d = 0.5\sin(0.6t)$.

The actuator fault model is defined as follows:

$$u = \begin{cases} v & \text{if } t < 10 \\ 0.2 + 0.8e^{-0.2t}\chi(v) + (\cos(\zeta_1))^2\zeta_2 & \text{if } t \geq 10 \end{cases} \tag{73}$$

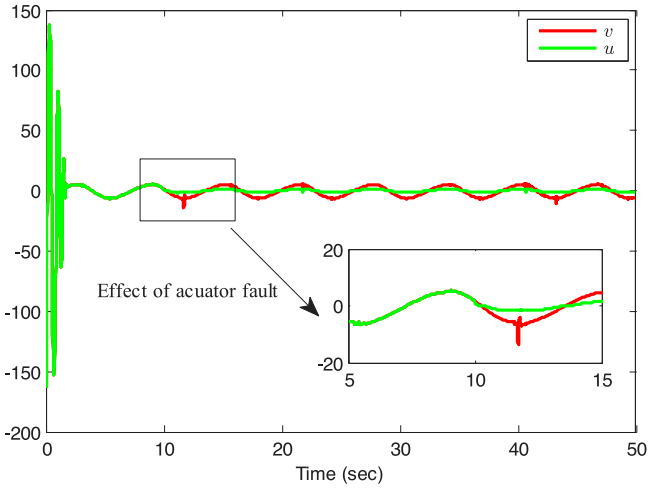

Fig. 9. The combine response of control input v and system input u.

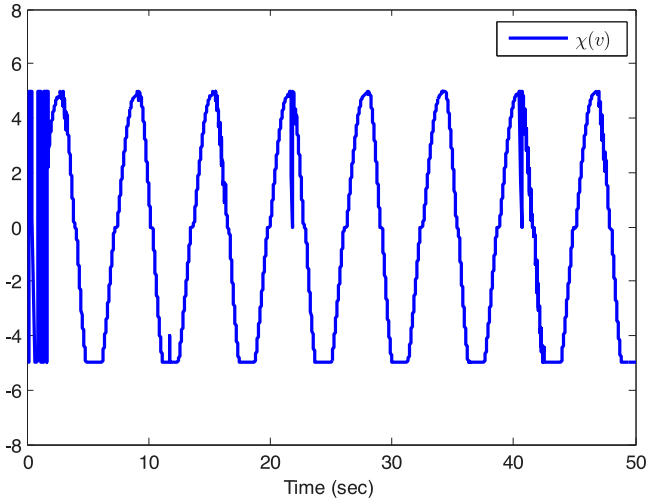

Fig. 10. The trajectory of input $\chi(v)$.

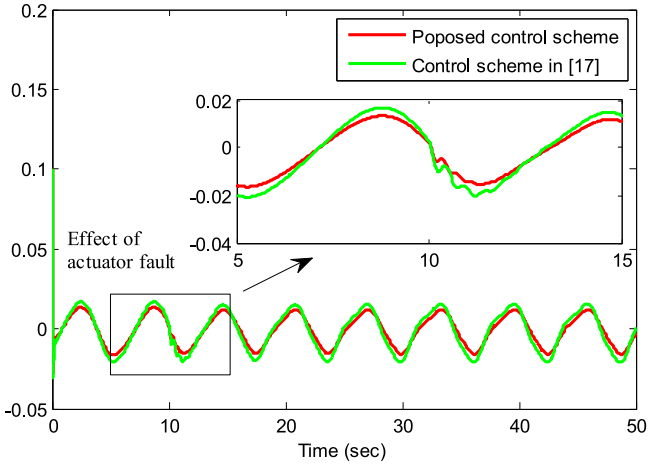

Fig. 11. Comparison of proposed method and existing method [17] based on the tracking error e_1.

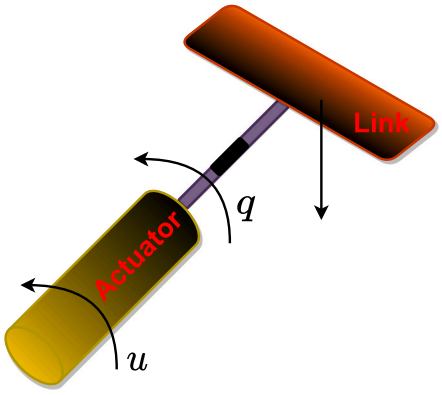

Fig. 12. One-link manipulator.

where $\rho(t,t_\rho) = 0.2 + 0.8e^{-0.2t}$, $u_r(t,t_r) = (\cos(\zeta_1))^2\zeta_2$, $t_0 = 10$ is the common time for both t_r and t_ρ. For $t < 10$, the fault model simplifies to $u = v$, indicating normal actuation and for $t \geq 10$, the actuator fault occurs.

The input $\chi(v)$ subjected to dead-zone and saturation is defined as

$$\chi(v) = \begin{cases} -40 & \text{if } v \leq -40 \\ \frac{40}{39.5}(v+0.5) & \text{if } -40 < v \leq -0.5 \\ 0 & \text{if } -0.5 < v \leq 0.8 \\ \frac{60}{59.2}(v-0.8) & \text{if } 0.8 < v \leq 60 \\ 60 & \text{if } v > 60 \end{cases} \tag{74}$$

From Theorem 1, the virtual control law α_i and actual control law v are chosen as

$$\alpha_i = -k_i e_i - \frac{1}{2\beta_i^2} e_i \hat{\theta}_i Q_i^T(Z_i) Q_i(Z_i), \quad i = 1, 2. \tag{75}$$

$$v = -k_3 e_3 - \frac{1}{2\beta_3^2 \rho_{\min}} e_3 \hat{\theta}_3 Q_3^T(Z_3) Q_3(Z_3). \tag{76}$$

The adaptive law is chosen as

$$\dot{\hat{\theta}}_i = \frac{b_i}{2\beta_i^2} e_i^2 Q_i^T(Z_i) Q_i(Z_i) - \varrho_i \hat{\theta}_i, \quad i = 1, 2, 3. \tag{77}$$

In the simulation, the initial conditions are chosen as $[\zeta_1(0), \zeta_2(0), \zeta_3(0)]^T = [0.5, 0.5, 0.5]^T$, $[\hat{\theta}_1(0), \hat{\theta}_2(0), \hat{\theta}_3(0)]^T = [0, 0, 0]^T$. Additionally, the design parameters are chosen by trial-and-error method as $k_1 = 10, k_2 = 10, k_3 = 20$, $\beta_1 = 2, \beta_2 = 2, \beta_3 = 2$, $b_1 = 0.5, b_2 = 0.5, b_3 = 0.5$, $\varrho_1 = 0.05, \varrho_2 = 0.05, \varrho_3 = 0.05$. The centre and width of the RBFNN are chosen by trial-and-error method as $\mu_i = [-2, 2]$ and $\nu_i = 2$ for $i = 1, 2, 3$.

Simulation results shown in Figs. 13 to 21 confirm the effectiveness of the closed-loop system. Fig. 13 displays both the system output y and the reference signal y_d. The tracking error e_1 is shown in Fig. 14, which clearly indicates that the tracking error is bounded. A closer look within Fig. 14 reveals the impact of actuator faults for $t \geq 10$. Fig. 15 highlights the bounded behavior of the state variables ζ_2 and ζ_3. The adaptive parameter response curves, which remain bounded, are displayed in Fig. 16. Fig. 17 displays the plot of the control input v, while Fig. 18 depicts the plot of the system input u. The combined plots of v and u are shown in Fig. 19. A zoomed-in view in Fig. 19 again highlights the effect of actuator faults for $t \geq 10$. Fig. 20 depicts the input $\chi(v)$. To showcase the advantages of the proposed adaptive control scheme, we compared it to an existing control method [17]. Fig. 21 shows the comparative results based on the tracking error $e_1 = y - y_d$, demonstrating that the proposed method slightly outperforms the existing control method [17]. Overall, the simulation results confirm that all signals within the closed-loop system remain bounded, indicating excellent tracking performance.

As in Example 1, we conducted a comparison to highlight the advantages of our proposed adaptive control method over the existing method [17]. The results are shown in Table 2, where it is clear that our proposed method outperforms the existing method [17]. Despite the challenges posed by actuator faults, dead-zone, and saturation, our approach delivers superior performance. This demonstrates the practicality and effectiveness of our proposed control strategy.

5. Conclusion

This research focuses on adaptive fault-tolerant neural control for strict-feedback nonlinear systems affected by actuator faults, dead-zones, and saturation. The proposed approach introduces an adaptive fault-tolerant controller that incorporates the

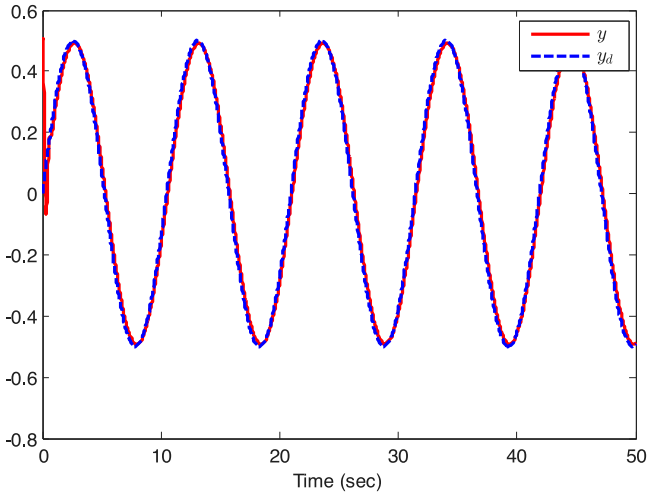

Fig. 13. Trajectories of y and y_d.

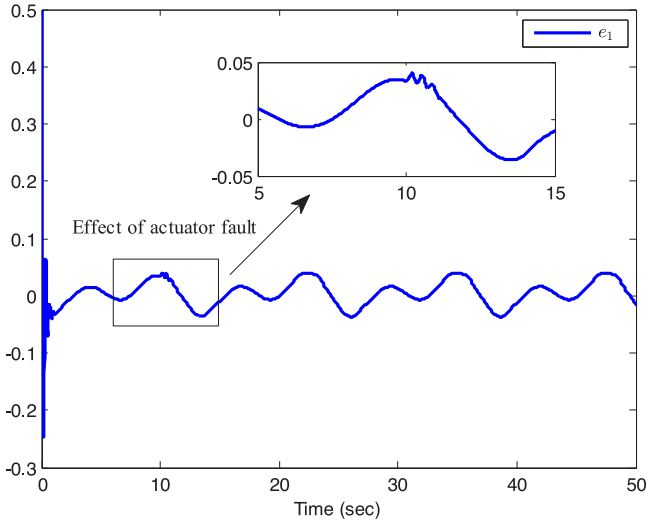

Fig. 14. The response of tracking error $e_1 = y - y_d$.

Table 2
Performance comparison of control methods.

Performance indices	Proposed method	Ref. [17]
ITAE	26.1224	30.7926
RMSE	0.0339	0.0421
MAE	0.0224	0.0273

backstepping technique and utilizes radial basis function neural networks (RBFNNs) for approximation. By applying Lyapunov stability theory, the controller ensures precise tracking of the reference signal by the system output with small bounded error, while ensuring that all signals within the closed-loop system remain bounded. Simulation results are presented to illustrate the effectiveness of this approach. Future research will expand adaptive fault-tolerant control methods to tackle the control challenges posed by more complex systems, including higher-order stochastic systems and nonstrict-feedback switched nonlinear systems with unmeasured states. Furthermore, validating the effectiveness and applicability of the proposed control methodology on both a quadrotor and a 6-link manipulator will be crucial in practical scenarios.

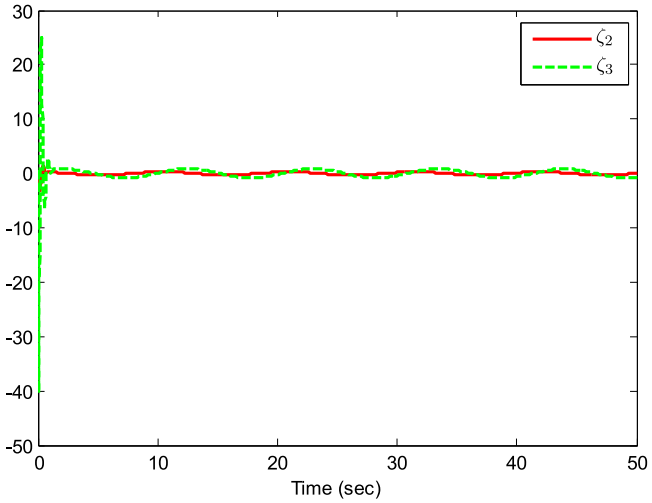

Fig. 15. The trajectories of state variables ζ_2 and ζ_3.

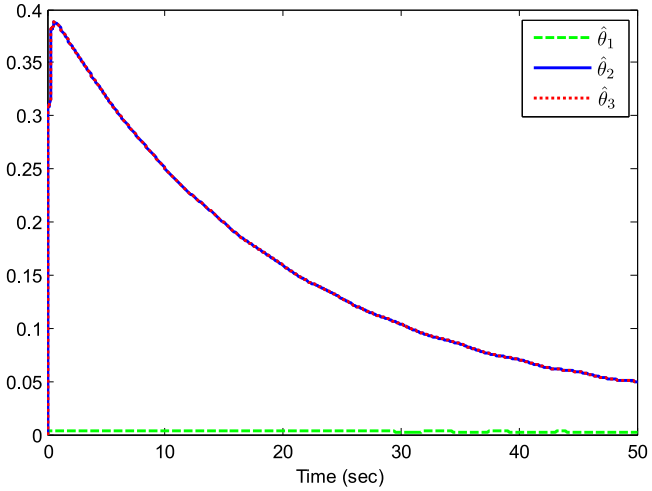

Fig. 16. The trajectories of adaptive laws.

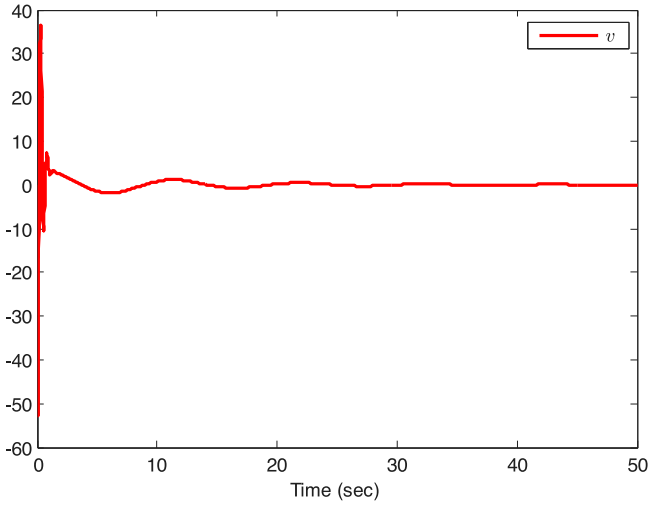

Fig. 17. Trajectory of control input v.

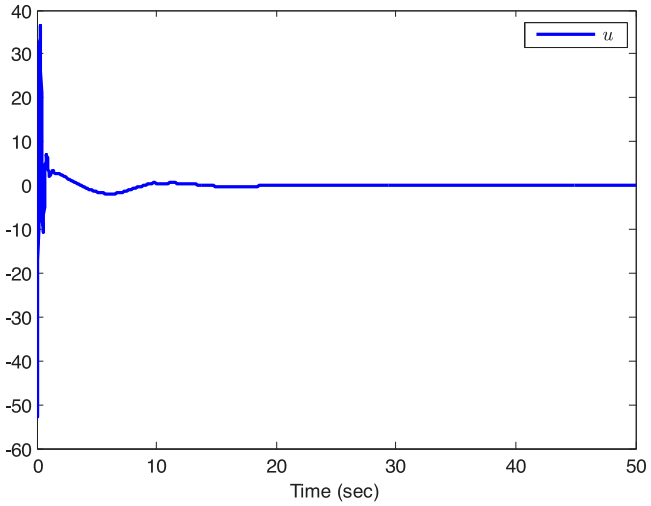

Fig. 18. Trajectory of system input u.

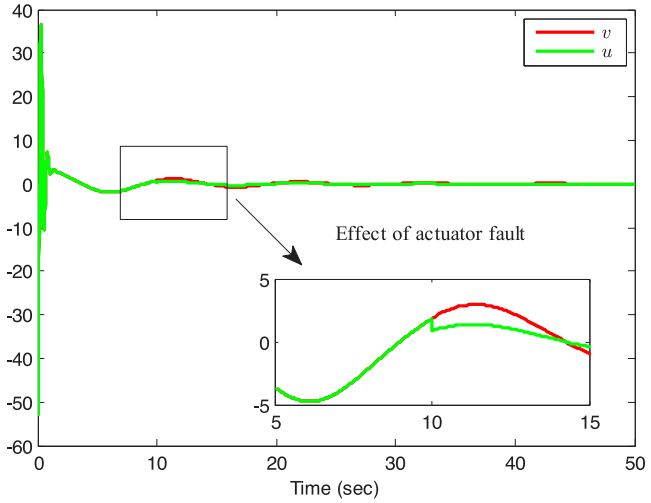

Fig. 19. The combine response of control input v and system input u.

CRediT authorship contribution statement

Mohamed Kharrat: Writing – original draft, Visualization, Validation, Supervision, Software, Methodology, Investigation, Funding acquisition, Formal analysis, Data curation, Conceptualization. **Moez Krichen:** Writing – original draft, Visualization, Validation, Supervision, Software, Project administration, Methodology, Investigation, Formal analysis, Data curation, Conceptualization. **Hadil Alhazmi:** Writing – original draft, Visualization, Validation, Supervision, Methodology, Investigation, Formal analysis, Data curation, Conceptualization. **Paolo Mercorelli:** Writing – original draft, Supervision, Resources, Project administration, Methodology, Investigation, Funding acquisition, Formal analysis, Data curation, Conceptualization.

Declaration of competing interest

The authors declare that they have no known competing financial interests or personal relationships that could have appeared to influence the work reported in this paper.

Acknowledgment

This work was funded by the Deanship of Graduate Studies and Scientific Research at Jouf University under grant No. (DGSSR-2024-02-01008).

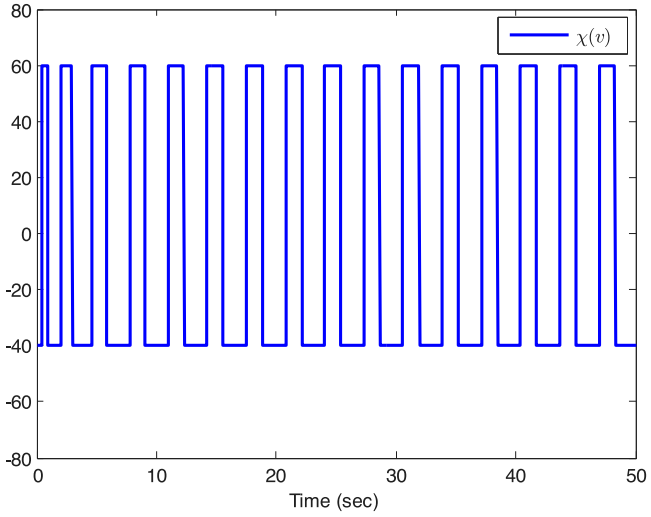

Fig. 20. Trajectory of input $\chi(v)$.

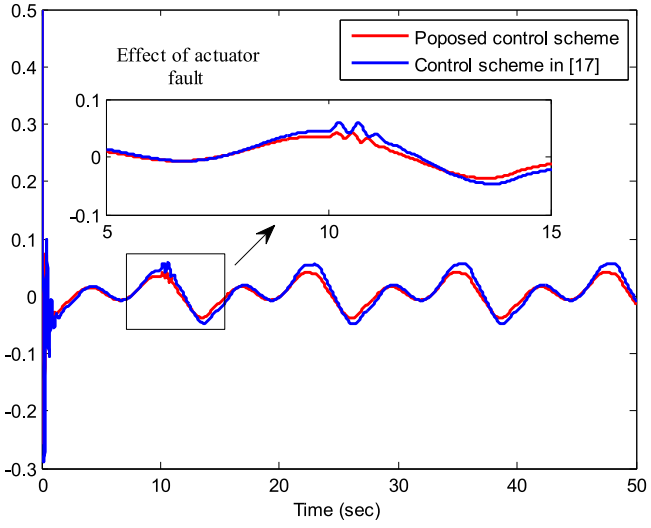

Fig. 21. Comparison of proposed method and existing method [17] based on the tracking error e_1.

Data availability

No underlying data was collected or produced in this study.

References

[1] Z. Yang, X. Zhang, X. Zong, G. Wang, Adaptive fuzzy control for non-strict feedback nonlinear systems with input delay and full state constraints, J. Frank. Inst. 357 (2020) 6858–6881.
[2] X.Y. Zheng, Adaptive neural control for non-strict feedback stochastic nonlinear systems with input delay, Trans. Inst. Meas. Control 46 (2024) 104–115.
[3] M. Kharrat, M. Krichen, L. Alkhalifa, K. Gasmi, Neural networks-based adaptive command filter control for nonlinear systems with unknown backlash-like hysteresis and its application to single link robot manipulator, AIMS Math. 9 (2024) 959–973.
[4] T. Yu, Y.J. Liu, L. Liu, Adaptive neural control for nonlinear MIMO function constraint systems, IEEE/CAA J. Autom. Sin. 10 (2023) 816–818.
[5] T. Gao, T. Li, Y.J. Liu, S. Tong, IBLF-based adaptive neural control of state-constrained uncertain stochastic nonlinear systems, IEEE Trans. Neural Netw. Learn. Syst. 33 (2021) 7345–7356.
[6] Y.X. Li, M. Wei, S. Tong, Event-triggered adaptive neural control for fractional-order nonlinear systems based on finite-time scheme, IEEE Trans. Cybern. 52 (2021) 9481–9489.
[7] P. Ju, Y. Ju, J. Song, Fuzzy adaptive asymptotic control for a class of large-scale high-order unknown nonlinear systems, Appl. Sci. 13 (2023) 8968.

[8] K. Xu, H. Wang, P.X. Liu, Adaptive fuzzy finite-time tracking control of nonlinear systems with unmodeled dynamics, Appl. Math. Comput. 450 (2016) 127992.
[9] L. Liu, T. Gao, Y.J. Liu, S. Tong, Time-varying asymmetrical BLFs based adaptive finite-time neural control of nonlinear systems with full state constraints, IEEE/CAA J. Autom. Sin. 7 (2020) 1335–1343.
[10] J. Xia, J. Zhang, W. Sun, B. Zhang, Z. Wang, Finite-time adaptive fuzzy control for nonlinear systems with full state constraints, IEEE Trans. Syst. Man Cybern. Syst. 49 (2018) 1541–1548.
[11] J. Xia, J. Zhang, J. Feng, Z. Wang, S. Zhuang, Command filter-based adaptive fuzzy control for nonlinear systems with unknown control directions, IEEE Trans. Syst. Man Cybern. Syst. 51 (2019) 1945–1953.
[12] M. Chen, H. Wang, X. Liu, Adaptive fuzzy practical fixed-time tracking control of nonlinear systems, IEEE Trans. Fuzzy Syst. 29 (2019) 664–673.
[13] Y.J. Huang, T.C. Kuo, S.H. Chang, Ast finite time fractional-order robust-adaptive sliding mode control of nonlinear systems with unknown dynamics, J. Comput. Appl. Math. 438 (2024) 115554.
[14] H. Wang, P.X. Liu, X. Zhao, X. Liu, Adaptive fuzzy finite-time control of nonlinear systems with actuator faults, IEEE Trans. Cybern. 50 (2019) 1786–1797.
[15] M. Kharrat, M. Krichen, L. Alkhalifa, K. Gasmi, Neural-networks-based adaptive fault-tolerant control of nonlinear systems with actuator faults and input quantization, IEEE Access 11 (2023) 137680-137687.
[16] N. Sheng, Z. Ai, J. Tang, Fuzzy adaptive command filtered backstepping fault-tolerant control for a class of nonlinear systems with actuator fault, J. Frank. Inst. 358 (2021) 6526–6544.
[17] W. Liu, F. Xie, Backstepping-based adaptive control for nonlinear systems with actuator failures and uncertain parameters, Circuits Syst. Signal Process. 39 (2020) 138–153.
[18] X. Deng, C. Zhang, Y. Ge, Adaptive neural network dynamic surface control of uncertain strict-feedback nonlinear systems with unknown control direction and unknown actuator fault, J. Frank. Inst. 359 (2022) 4054–4073.
[19] L.X. Xu, Y.L. Wang, X. Wang, C. Peng, Decentralized event-triggered adaptive control for interconnected nonlinear systems with actuator failures, IEEE Trans. Fuzzy Syst. 31 (2022) 148–159.
[20] M. Kharrat, Adaptive fault-tolerant control for a class of nonstrict-feedback nonlinear systems with unmodeled dynamics and dead-zone output using multi-dimensional taylor networks, Nonlinear Dynam. 112 (2024) 13289–13306.
[21] Y.H. Jing, G.H. Yang, Fuzzy adaptive fault-tolerant control for uncertain nonlinear systems with unknown dead-zone and unmodeled dynamics, IEEE Trans. Fuzzy Syst. 27 (2019) 2265–2278.
[22] L. Liu, Y.J. Liu, S. Tong, Neural networks-based adaptive finite-time fault-tolerant control for a class of strict-feedback switched nonlinear systems, IEEE Trans. Cybern. 49 (2018) 2536–2545.
[23] K. Lu, Z. Liu, Y. Wang, C.P. Chen, Resilient adaptive neural control for uncertain nonlinear systems with infinite number of time-varying actuator failures, IEEE Trans. Cybern. 52 (2020) 4356–4369.
[24] Y. Li, K. Sun, S. Tong, Observer-based adaptive fuzzy fault-tolerant optimal control for SISO nonlinear systems, IEEE Trans. Cybern. 49 (2018) 2978.
[25] S. Yin, H. Yang, H. Gao, J. Qiu, O. Kaynak, An adaptive NN-based approach for fault-tolerant control of nonlinear time-varying delay systems with unmodeled dynamics IIEEE trans, Neural Netw. Learn. Syst. 28 (2016) 1902–1913.
[26] G. Xue, F. Lin, S. Li, H. Liu, Adaptive fuzzy finite-time backstepping control of fractional-order nonlinear systems with actuator faults via command-filtering and sliding mode technique, IEEE Trans. Cybern. 600 (2022) 189–208.
[27] Z. Zhang, S. Xu, B. Zhang, Exact tracking control of nonlinear systems with time delays and dead-zone input, IEEE Trans. Cybern. 52 (2015) 272–276.
[28] Z. Li, T. Li, G. Feng, R. Zhao, Q. Shan, Neural network-based adaptive control for pure-feedback stochastic nonlinear systems with time-varying delays and dead-zone input, IEEE Trans. Syst. Man Cybern. Syst. 50 (2018) 5317–5329.
[29] Y.Q. Han, Adaptive tracking control of a class of nonlinear systems with unknown dead-zone output: a multi-dimensional taylor network (MTN)-based approach, Internat. J. Control 94 (2021) 3161–3170.
[30] K. He, C. Dong, Q. Wang, Active disturbance rejection adaptive control for uncertain nonlinear systems with unknown time-varying dead-zone input, Asian J. Control 24 (2022) 1209–1222.
[31] X. Su, Z. Liu, G. Lai, Event-triggered robust adaptive control for uncertain nonlinear systems preceded by actuator dead-zone, Nonlinear Dynam. 93 (2018) 219–231.
[32] H. Li, L. Bai, L. Wang, Q. Zhou, H. Wang, Adaptive neural control of uncertain nonstrict-feedback stochastic nonlinear systems with output constraint and unknown dead zone, IEEE Trans. Syst. Man Cybern. Syst. 47 (2016) 2048–2059.
[33] G. Lai, G. Tao, Y. Zhang, Z. Liu, Adaptive control of noncanonical neural-network nonlinear systems with unknown input dead-zone characteristics, IEEE Trans. Neural Netw. Learn. Syst. 31 (2019) 3346–3360.
[34] K. Yu, Y. Li, Fuzzy adaptive event-triggered output feedback control for nonlinear systems with tracking error constrained and unknown dead-zone, Int. J. Syst. Sci. 52 (2021) 2918–2933.
[35] J. Lan, Y.J. Liu, L. Liu, S. Tong, Adaptive output feedback tracking control for a class of nonlinear time-varying state constrained systems with fuzzy dead-zone input, IEEE Trans. Fuzzy Syst. 29 (2022) 1841–1852.
[36] M.H. Rezaei, M. Ghaseminezhad, M. Kabiri, Control of uncertain non-affine nonlinear systems using neural networks subject to input saturation with unknown control direction, J. Vib. Control (2024) 10775463241273826.
[37] N. Zerari, M. Chemachema, Event-triggered adaptive output-feedback neural-networks control for saturated strict-feedback nonlinear systems in the presence of external disturbance, Nonlinear Dynam. 104 (2021) 1343–1362.
[38] Y. Wu, X.J. Xie, Robust adaptive control for state-constrained nonlinear systems with input saturation and unknown control direction, I IEEE Trans. Syst. Man Cybern. Syst. 159 (2015) 117–125.
[39] M. Iqbal, M. Rehan, K.S. Hong, A. Khaliq, Sector-condition-based results for adaptive control and synchronization of chaotic systems under input saturation, Chaos, Solitons and Fractals 77 (2015) 158–169.
[40] X. Yan, M. Chen, G. Feng, Q. Wu, S. Shao, Fuzzy robust constrained control for nonlinear systems with input saturation and external disturbances, IEEE Trans. Fuzzy Syst. 29 (2019) 345–356.
[41] L. Edalati, A.K. Sedigh, M.A. Shooredeli, A. Moarefianpour, Adaptive fuzzy dynamic surface control of nonlinear systems with input saturation and time-varying output constraints, Mech. Syst. Signal Process. 100 (2018) 311–329.
[42] G. Cui, J. Yu, Q.G. Wang, Finite-time adaptive fuzzy control for MIMO nonlinear systems with input saturation via improved command-filtered backstepping, IEEE Trans. Syst. Man Cybern. Syst. 52 (2020) 980–989.
[43] S. Sui, S. Tong, Y. Li, Observer-based fuzzy adaptive prescribed performance tracking control for nonlinear stochastic systems with input saturation, Neurocomputing 158 (2015) 100–108.
[44] A. Chen, L. Tang, Y.J. Liu, Y. Gao, Adaptive control for switched uncertain nonlinear systems with time-varying output constraint and input saturation, Internat. J. Adapt. Control Signal Process. 33 (2019) 1344–1358.
[45] Q. Zhou, C. Wu, P. Shi, Observer-based adaptive fuzzy tracking control of nonlinear systems with time delay and input saturation, Neurocomputing 316 (2017) 49–68.
[46] S. Kang, P.X. Liu, H. Wang, Fixed-time adaptive fuzzy command filtering control for a class of uncertain nonlinear systems with input saturation and dead zone, Nonlinear Dynam. 110 (2022) 2401–2414.

[47] X. Zhou, C. Gao, Z.G. Li, X.Y. Ouyang, L.B. Wu, Observer-based adaptive fuzzy finite-time prescribed performance tracking control for strict-feedback systems with input dead-zone and saturation, Nonlinear Dynam. 103 (2021) 1645–1661.
[48] G. Zong, Q. Xu, X. Zhao, S.F. Su, L. Song, Output-feedback adaptive neural network control for uncertain nonsmooth nonlinear systems with input deadzone and saturation, IEEE Trans. Cybern. 53 (2022) 5957–5969.
[49] A. Kamalamiri, M. Shahrokhi, M. Mohit, Adaptive finite-time neural control of non-strict feedback systems subject to output constraint, unknown control direction, and input nonlinearities, Inform. Sci. 520 (2020) 271–291.
[50] L. Liu, Y.J. Liu, A. Chen, S. Tong, C.P. Chen, Integral barrier Lyapunov function-based adaptive control for switched nonlinear systems, Sci. China Inf. Sci. 63 (2020) 1–14.
[51] D. Cui, C.K. Ahn, Z. Xiang, Fault-tolerant fuzzy observer-based fixed-time tracking control for nonlinear switched systems, IEEE Trans. Fuzzy Syst. 31 (2023) 4410–4420.
[52] D. Cui, M. Chadli, Z. Xiang, Fuzzy fault-tolerant predefined-time control for switched systems: a singularity-free method, IEEE Trans. Fuzzy Syst. 32 (2023) 1223–1232.
[53] D. Cui, C.K. Ahn, Y. Sun, Z. Xiang, Mode-dependent state observer-based prescribed performance control of switched systems, IEEE Trans. Circuits Syst. II: Express Briefs (2024).
[54] X. Wang, J. Xu, M. Lv, L. Zhang, Z. Zhao, Barrier Lyapunov function-based fixed-time FTC for high-order nonlinear systems with predefined tracking accuracy, Nonlinear Dynam. 110 (1) (2022) 381–394.
[55] Y. Liu, Q. Zhu, Adaptive fuzzy finite-time control for nonstrict-feedback nonlinear systems, IEEE Trans. Cybern. 52 (2021) 10420–10429.